Journal of Magnetism and Magnetic Materials 360 (2014) 200–204

Contents lists available at ScienceDirect

Journal of Magnetism and Magnetic Materials

journal homepage: www.elsevier.com/locate/jmmm

Magnetic order of the La_3NiGe_2-type Ho_3NiGe_2

A.V. Morozkin [a,*], Jinlei Yao [b], Fang Yuan [b], Y. Mozharivskyj [b], O. Isnard [c,d]

[a] Department of Chemistry, Moscow State University, GSP-2, Leninskie Gory, House 1, Building 3, Moscow 119992, Russia
[b] Department of Chemistry and Chemical Biology, McMaster University, 1280 Main Street West, Hamilton, Ontario, Canada, L8S 4M1
[c] Université Grenoble Alpes, Inst NEEL, BP166, F-38042 Grenoble, France
[d] CNRS, Institut NEEL, 25 rue des martyrs, F-38042 Grenoble, France

ARTICLE INFO

Available online 20 February 2014

Keywords:
Rare earth intermetallics
Neutron diffraction
Magnetic structure

ABSTRACT

Magnetic measurements and neutron powder diffraction investigation of the magnetic structure of the La_3NiGe_2-type Ho_3NiGe_2 compound are presented. It is found that below T_C=43 K Ho_3NiGe_2 exhibits a commensurate *ac*-plane mixed antiferromagnetic–ferromagnetic ordering with **Pn'ma** magnetic space group. At 1.5 K the holmium magnetic moment reaches the value of 9.1(2)μ_B.

1. Introduction

The Ho_3NiGe_2 compound crystallizes in the La_3NiGe_2-type (space group *Pnma*) structure. The La_3NiGe_2 structure is a member of the family of the two-layer orthorhombic structures with the *Pnma* symmetry and a set of special 4*c* sites (*x*, 1/4, z) derived from the hexagonal Mg structure [1].

The La_3NiGe_2-type $\{Pr, Nd\}_3CoGe_2$ have been shown as a mixed antiferromagnetic–ferromagnetic *ac*-plane ordering with the **Pn'ma** magnetic space group ordering [2], whereas Tb_3NiGe_2 compound demonstrates a *b*-axis ferrimagnetic ordering with the **Pnm'a** magnetic space group [3] (Fig. 1).

This work aims to understand the nature of the magnetic ordering in Ho_3NiGe_2 isostructural compound via magnetic and neutron diffraction study.

2. Experimental details

The Ho_3NiGe_2 sample was prepared by arc-melting the weighed amounts of holmium (99.9 wt%), nickel (99.95 wt%) and germanium (99.99 wt%). The sample was annealed at 1070 K for 175 h in an argon atmosphere and quenched in ice-cold water.

The quality of the samples was evaluated using powder X-ray diffraction (XRD) and X-ray spectral microprobe analysis. The XRD data were obtained on a DRON-3.0 diffractometer (CuK_α radiation, 2Θ=5–120°, step 0.02°, 8 s per step) at room temperature. The unit cell data were derived using the Rietan-program [4] in the isotropic approximation. A «Camebax» microanalyser was employed to perform microprobe X-ray spectral analysis of the samples (15 kV, 3×10^{-8} A, *K*-, *L*- and *M*- lines, 2×2 μm^2).

The temperature-dependant dc magnetization and saturation magnetization were measured on a commercial SQUID magnetometer (Quantum Design) in the 5–300 K range and in an applied field of up to 50 kOe.

The neutron diffraction experiments were carried out on the D1B powder diffractometer [5] (λ=0.252 nm at the Institute Laue-Langevin, Grenoble, France). The neutron diffraction patterns were identified and calculated using the FULLPROF-program and traditional crystallographic approach [6].

3. Results

3.1. Crystal structure

The quantitative microprobe X-ray analysis of the Ho_3NiGe_2 sample yielded the $Ho_{50}Ni_{17}Ge_{33}$ composition which is identical to the expected one. The structural parameters of La_3NiGe_2-type Ho_3NiGe_2 are given in Table 1. The interatomic distances of Ho_3NiGe_2 are close to the sum of metallic ratio [7] and, thus, are indicative of the metallic type bonding in the structure (Table 2).

The plots for the dc magnetization and inverse susceptibility of the polycrystalline Ho_3NiGe_2 sample are given in Fig. 2a. According to the magnetization data, Ho_3NiGe_2 undergoes a ferromagnetic-type transition at 43 K. The paramagnetic susceptibility follows the Curie–Weiss law in the temperature range from 60 to 300 K. The fit to the Curie–Weiss law in this region gives a positive Weiss temperature Θ_p=30.2 K suggesting dominant ferromagnetic interactions. The effective magnetic moments per formula unit M_{eff}/f.u.

* Corresponding author
E-mail address: morozkin@general.chem.msu.ru (A.V. Morozkin).

http://dx.doi.org/10.1016/j.jmmm.2014.02.038
0304-8853

of 18.37 μ_B $\mu_B$yields an effective magnetic moment of 10.61 μ_B per Ho atom which is in good agreement with the theoretical value of 10.607 μ_B for Ho^{3+} [8] (Fig. 2a). These data also suggest that Ni atoms carry no magnetic moment a feature known to be frequently observed in rare-earth rich nickel intermetallics as well as in other R-Ni-Ge compounds [12].

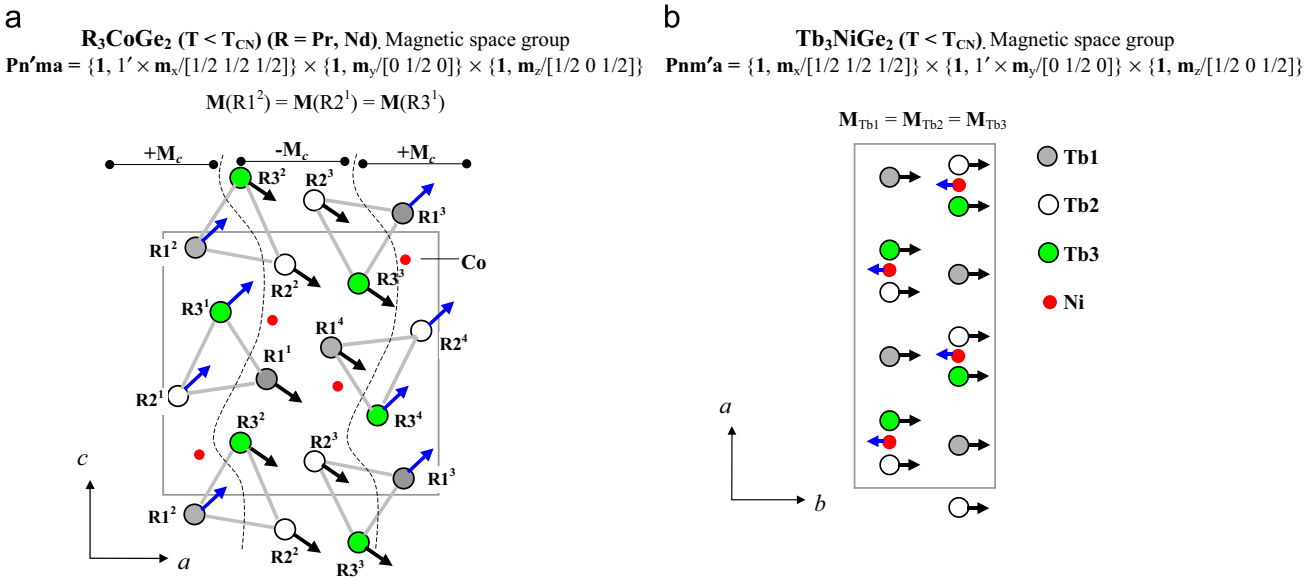

Fig. 1. Magnetic structure of (a) Pr_3CoGe_2 and Nd_3CoGe_2 (mixed antiferromagnetic–ferromagnetic ordering with the **Pn'ma** magnetic space group) [2] and (b) of Tb_3NiGe_2 (ferrimagnetic with the **Pnm'a** magnetic space group) [3]. The area of ferromagnetically ordered rare-earth atoms '+$\mathbf{M}_c$' and '-$\mathbf{M}_c$' is shown in Figure a.

Table 1
Atomic positions in the La_3NiGe_2-type Ho_3NiGe_2 structure (a=1.12991(6) nm, b=0.41530(2) nm, c=1.11466(6) nm, space group *Pnma, No. 62*, Z=4, atomic displacement parameters for all atoms β_{11}=0.001958, β_{22}=0.014495 and β_{33}=0.002012, R_F=3.7%, 298 K)[a].

Atom	Site	x/*a*	y/*b*	z/*c*	Occupancy
Ho1	*4c*	0.3775(3)	1/4	0.4411(3)	1.00
Ho2	*4c*	0.0532(3)	1/4	0.3746(3)	1.00
Ho3	*4c*	0.2117(3)	1/4	0.7007(5)	1.00
Ni	*4c*	0.1243(7)	1/4	0.1279(7)	1.00
Ge1	*4c*	0.4813(5)	1/4	0.6805(6)	1.00
Ge2	*4c*	0.3093(5)	1/4	0.0077(7)	1.00

[a] The crystallographic data used with permission - © JCPDS - International Center for Diffraction Data.

Table 2
Interatomic distances for $Ho3NiGe_2$. Their ratio to the sum of the atomic radii of the corresponding atoms [7] is given as $\Delta = D/(R_{atom1}+R_{atom2})$. δ is a coordination number. The shortest Ho–Ho distances are highlighted in bold.

Atom-	Atom	D, Å	Δ	Atom-	Atom	D, Å	Δ	Atom-	Atom	D, Å	Δ
Ho1 -	1Ni	0.28927	0.96	Ho2 -	1Ni	0.28648	0.95	Ho3 -	2Ni	0.28990	0.96
	1Ge1	0.29149	0.97		2Ge2	0.29878	1.00		1Ge1	0.29208	0.98
	2Ni	0.29407	0.98		2Ge1	0.30240	1.01		2Ge2	0.29994	1.00
	1Ge1	0.29486	0.99		1Ge2	0.30522	1.02		1Ge1	0.30545	1.02
	2Ge2	0.30525	1.02		2Ho2[a]	**0.36841**	**1.04**		1Ho1[a]	**0.34472**	**0.98**
	1Ho3[a]	**0.34472**	**0.98**		2Ho3	0.37383	1.06		2Ho1	0.35367	1.00
	2Ho3	0.35367	1.00		1Ho1[a]	0.37385	1.06		1Ge2	0.35953	1.20
	2Ho1	0.37013	1.05		2Ho3	0.38892	1.10		2Ho2	0.37383	1.06
	1Ho2[a]	0.37385	1.06		1Ho1	0.40404	1.14		2Ho2	0.38892	1.10
	1Ho2	0.40404	1.14		1Ho3a	0.40521	1.15		1Ho2a	0.40521	1.15
	2Ho1	0.41530	1.18		2Ho2	0.41530	1.18		2Ho3	0.41530	1.18
		***δ*=16**				***δ*=17**				***δ*=17**	
Ni^- -	2Ge1	0.24656	1.00	$Ge1^-$-	2Ni	0.24656	1.00	Ge2 -	1Ni	0.24829	1.00
	1Ge2	0.24829	1.00		1Ho1	0.29149	0.97		2Ho2	0.29878	1.00
	1Ho2	0.28648	0.95		1Ho3	0.29208	0.98		2Ho3	0.29994	1.00
	1Ho1	0.28927	0.96		2Ho1	0.29486	0.99		1Ho2	0.30522	1.02
	2Ho3	0.28990	0.96		1Ho2	0.30240	1.01		2Ho1	0.30525	1.02
	1Ho1	0.29407	0.98		1Ho3	0.30545	1.02		1Ho3	0.35953	1.20
		***δ*=12**				***δ*=12**				***δ*=12**	

[a] Bonds shown in Fig. 5.

The magnetization vs. field data at 5 K of Ho_3NiGe_2 are plotted in Fig. 2b. The weak slope change around 18 kOe may correspond to the metamagnetic-like transition in Ho_3NiGe_2 at 5 K. Meanwhile, both non-saturating behavior and relatively low magnetization values at 50 kOe (23.3 μ_B/f.u. and 7.8 μ_B/Ho) suggest a disordered ferromagnetic state or presence of antiferromagnetic interactions in its magnetic ordering. In order to probe such hypothesis we have undertaken powder neutron diffraction experiments at low temperature to determine the magnetic ordering.

3.2. Neutron diffraction study of La_3NiGe_2-type Ho_3NiGe_2

The La_3NiGe_2-type Ho_3NiGe_2 structure (space group *Pnma*, point group $\mathbf{D}_{2h}$) consists of the *4c* sites for the holmium, nickel and germanium atoms (Table 1). Such two-layer structure with the *Pnma* space group may be given in terms of the orthorhombic $Pna2_1$ (point group $\mathbf{C}_{2v}$), $P2_12_12_1$ (point group $\mathbf{D}_2$) or monoclinic $P2_1/n$ (point group $\mathbf{C}^x_{2h}$) and $P2_1/a$ (point group $\mathbf{C}^z_{2h}$) space groups in case of the orthorhombic ($y/b = 1/4 \rightarrow y/b \neq 1/4$) or monoclinic distortion of the unit cell. The symmetry operators for the corresponding point and space groups and *4c* atomic positions of the holmium sublattice are given in Table 3. These "colorless" $\mathbf{D}_2$, $\mathbf{C}_{2h}$ and $\mathbf{C}_{2v}$ point groups and "black–white" $\mathbf{D}_2'$, $\mathbf{C}_{2h}'$ and $\mathbf{C}_{2v}'$ magnetic point groups [9–11] were used for the analysis of the observed neutron diffraction data.

The analysis of the thermal dependence of the diffraction pattern reveals that the unit cell of Ho_3NiGe_2 undegoes isotropic compression down to 63 K ($\Delta a/a_{291K} \approx \Delta b/b_{291K} \approx \Delta c/c_{291K} \approx -0.0021$ and $\Delta V/V_{291K} = -0.00643$ at 63 K) and anisotropic one below the

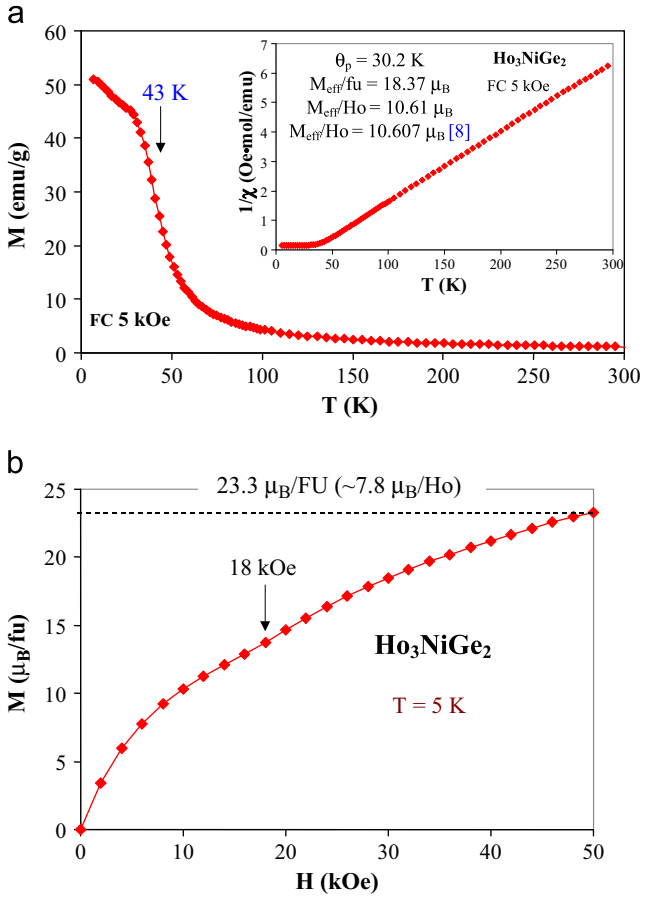

Fig. 2. (a) Magnetization and inverse magnetic susceptibility as a function of temperature in a 5 kOe field and (b) magnetization vs. field at 5 K for Ho_3NiGe_2.

Table 3
Atomic positions of the *4c* sites of space group *Pnma* [a] (retained by Ho_3NiGe_2 compound) with the corresponding symmetry operators and subgroups.

N	Atom	x/a	y/b	z/c	Symmetry operator	Point subgroup of *4c* site			
						D_2 [b]	C_{2v} [c]	C_{2h} [d]	C_{2h} [e]
1	$Ho1^1$, $Ho2^1$, $Ho3^1$	x	1/4	z	{**1**, $\mathbf{m}_y$/[0 1/2 0]}	**1**	**1**	**1**	**1**
2	$Ho1^2$, $Ho2^2$, $Ho3^2$	1/2 - x	3/4	1/2+z	{$\mathbf{2}_z$/[1/2 0 1/2], $\boldsymbol{m}_x$/[1/2 1/2 1/2]}	$\mathbf{2}_z$	$\mathbf{m}_x$	$\boldsymbol{m}_x$	$\mathbf{2}_z$
3	$Ho1^3$, $Ho2^3$, $Ho3^3$	1/2+x	1/4	1/2 - z	{$\mathbf{m}_z$/[1/2 0 1/2], $\mathbf{2}_x$/[1/2 1/2 1/2]}	$\mathbf{2}_x$	$\mathbf{m}_z$	$\mathbf{2}_x$	$\mathbf{m}_z$
4	$Ho1^4$, $Ho2^4$, $Ho3^4$	- x	3/4	- z	{$\bar{\mathbf{1}}$, $\mathbf{2}_y$/[0 1/2 0]}	$\mathbf{2}_y$	$\mathbf{2}_y$	$\bar{\mathbf{1}}$	$\bar{\mathbf{1}}$

[a] for two layers structure $Pnma(x, y, z) = \{\mathbf{1}, \mathbf{m}_y/[0\ 1/2\ 0]\} \times \{Pna2_1(x, y, z), P2_12_12_1(x, y, z), P2_1/n(x, y, z), P2_1/a(x, y, z)\}$.
[b] space group $P2_12_12_1 = \{\mathbf{1}, \mathbf{2}_x/[1/2\ 1/2\ 1/2], \mathbf{2}_y/[0\ 1/2\ 0], \mathbf{2}_z/[1/2\ 0\ 1/2]\}$.
[c] space group $Pna2_1 = \{\mathbf{1}, \boldsymbol{m}_x/[1/2\ 1/2\ 1/2], \mathbf{m}_z/[1/2\ 0\ 1/2], \mathbf{2}_y/[0\ 1/2\ 0]\}$.
[d] space group $P2_1/n = \{\mathbf{1}, \boldsymbol{m}_x/[1/2\ 1/2\ 1/2], \mathbf{2}_x/[1/2\ 1/2\ 1/2], \bar{\mathbf{1}}\}$.
[e] space group $P2_1/a = \{\mathbf{1}, \mathbf{m}_z/[1/2\ 0\ 1/2], \mathbf{2}_z/[1/2\ 0\ 1/2], \bar{\mathbf{1}}\}$.

ferromagnetic-type transition temperature of T_C=43 K: the *a* and *c* cell parameters decrease whereas the *b* one remains almost constant (Fig. 3). At 1.5 K the $\Delta a/a_{291K}$, $\Delta b/b_{291K}$ and $\Delta c/c_{291K}$ parameters reach the values of –0.00390, –0.00229 and –0.00323, respectively, whereas $\Delta V/V_{291K} = -0.00939$.

Based on the present powder neutron diffraction study, there are no obvious reasons to reduce the *Pnma* symmetry of the Ho_3NiGe_2 lattice to the $Pna2_1$, $P2_12_12_1$, $P2_1/n$ ore $P2_1/a$ ones as the temperature decreases from 291 K down to 1.5 K.

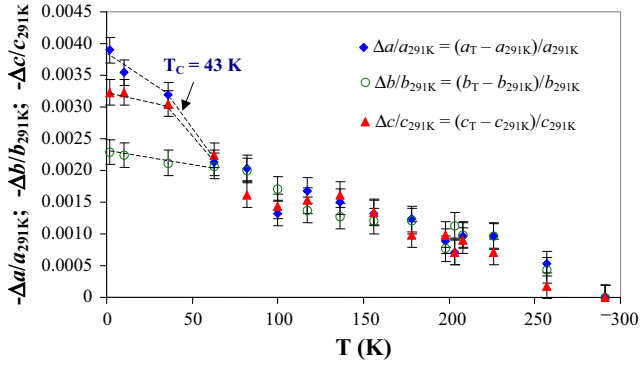

Fig. 3. The relative cell parameters of Ho_3NiGe_2 vs. temperature.

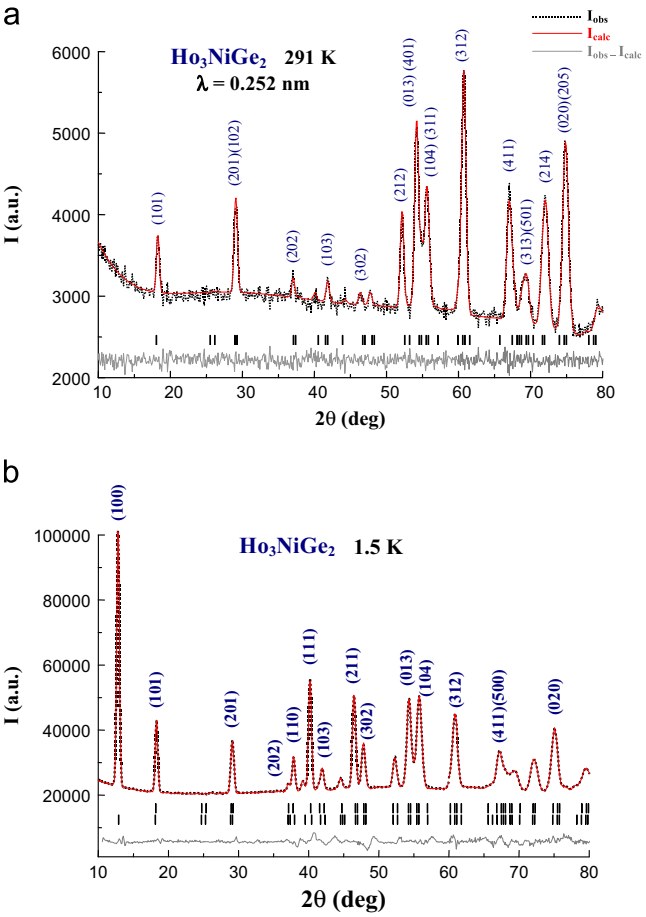

Fig. 4. Neutron diffraction patterns of Ho_3NiGe_2 (a) recorded at a wavelength of 0.252 nm and at 291 K (paramagnetic state) and (b) at 1.5 K (mixed antiferro–ferromagnetic ordering with the **Pn'ma** magnetic space group, wave vector $\mathbf{K}_0$=[0, 0, 0]). Strong magnetic reflections are shown in Figure b.

The set of commensurate magnetic reflections developing at 36 K was used to derive the magnetic ordering of Ho_3NiGe_2 (Fig. 4). The *ac*-plane magnetic structure with the **Pn'ma**=$\{\mathbf{1}, 1' \times \mathbf{m}_x/[1/2\ 1/2\ 1/2]\} \times \{\mathbf{1}, \mathbf{m}_y/[0\ 1/2\ 0]\} \times \{\mathbf{1}, \mathbf{m}_z/[1/2\ 0\ 1/2]\}$ magnetic space group with $\mathbf{M}(Ho1^1)=\mathbf{M}(Ho3^1)\neq\mathbf{M}(Ho2^1)$ was found to give the best agreement with the experimental data (Fig. 5 and Table 4). The '$Ho1^1$–$Ho3^{1'}$','$Ho1^2$–$Ho3^{2'}$','$Ho1^3$–$Ho3^{3'}$','$Ho1^4$–$Ho3^{4'}$','$Ho2^1$–$Ho2^{4'}$ and '$Ho2^2$–$Ho2^{3'}$ pairs with the shortest Ho–Ho distances (see Table 2) are observed to have collinear arrangement of their magnetic moments. At 1.4 K the holmium magnetic moments reach values of 9.1(2) μ_B that is somewhat smaller than the maximum 10 μ_B value expected for the free Ho^{3+} ion [8] (Table 4).

4. Discussion

The obtained magnetic structure of Ho_3NiGe_2 corresponds to the magnetic measurements: the behavoir of M–T curve corresponds to the mixed F–AF ordering (Fig. 2a), whereas a slope change around 18 kOe at 5 K in the field dependence of magnetization should correpond to the metamagnetic-like transition in present magnetic structure (Fig. 2b).

The magnetic structure of Ho_3NiGe_2 is similar to that of $\{Pr, Nd\}_3CoGe_2$ [2], however in contrast to the magnetic ordering in $\{Pr, Nd\}_3CoGe_2$, it does not have the ferromagnetically ordered '$+\boldsymbol{M}_c$' and '$-\boldsymbol{M}_c$' layers along the *a* axis (see Figs. 1a and 5). In [3] we suggested the possible magnetic ordering of Ni sublattice as the result of ferromagnetic ordering of Tb sublattice, because magnetic measurements and simple model of *b*-collinear magnetic structure do not contradict with such conclusion. Meanwhile, the structural features of La_3NiGe_2-type compounds complicate the magnetic ordering of the Ni (Co) sublattice and its possible contribution to the magnetic ordering of the present compounds corresponds to the estimated standard deviation (ESD) of magnetic structure's model. Therefore the magnetic ordering of rare earth sublattice plays a crucial role in magnetic properties of La_3NiGe_2-type compounds.

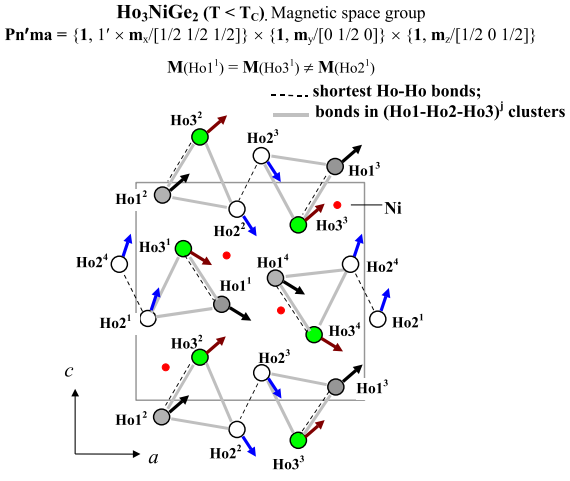

Fig. 5. Magnetic structure of Ho_3NiGe_2 (mixed antiferromagnetic–ferromagnetic ordering with the **Pn'ma** magnetic space group). The shortest Ho–Ho bonds ('$Ho1^1$–$Ho3^{1'}$','$Ho1^2$–$Ho3^{2'}$','$Ho1^3$–$Ho3^{3'}$','$Ho1^4$–$Ho3^{4'}$','$Ho2^1$–$Ho2^{4'}$ and '$Ho2^2$–$Ho2^{3'}$') and bonds of the '$Ho1^1$–$Ho2^1$–$Ho3^{1'}$','$Ho1^2$–$Ho2^2$–$Ho3^{2'}$','$Ho1^3$–$Ho2^3$–$Ho3^{3'}$' and '$Ho1^4$–$Ho2^4$–$Ho3^{4'}$' clusters are shown in Figure.

Table 4
Crystallographic and magnetic parameters of La_3NiGe_2-type Ho_3NiGe_2 at different temperatures: cell parameters; $\mathbf{M}_a$ and $\mathbf{M}_c$ are the Ho magnetic moments along the *a* and *c* axes, respectively; $|\mathbf{M}|$ is the magnitude of the holmium magnetic moment. Reliability factors are: R_F for the crystal structure and R_F^m for the magnetic structure.

T (K)	*a* (nm)	*b* (nm)	*c* (nm)	R_F (%)	Atom	M_a (μ_B)	M_c (μ_B)	$\|M\|$ (μ_B)	R_F^m (%)
298[a]	1.12991(6)	0.41530(2)	1.11466(6)	3.6					
291	1.1292(2)	0.41504(9)	1.1147(2)	4.7					
257	1.1286(2)	0.41486(9)	1.1145(3)	5.5					
226	1.1281(2)	0.41464(9)	1.1139(2)	5.8					
208	1.1281(2)	0.41463(7)	1.1137(2)	5.3					
203	1.1284(2)	0.41457(9)	1.1139(3)	5.2					
198	1.1282(2)	0.41472(9)	1.1136(2)	4.4					
178	1.1278(2)	0.41454(9)	1.1136(2)	5.5					
156	1.1277(2)	0.41454(9)	1.1132(2)	5.4					
136	1.1275(2)	0.41451(9)	1.1129(3)	5.6					
117	1.1273(3)	0.41447(9)	1.1130(3)	6.0					
100	1.1277(2)	0.41433(9)	1.1131(2)	5.4					
82	1.1269(2)	0.41421(9)	1.1129(2)	5.8					
63	1.1268(2)	0.41418(9)	1.1122(3)	5.6					
36	1.1256(2)	0.41416(5)	1.1113(2)	4.7	$Ho1^1$, $Ho1^4$, $Ho3^1$, $Ho3^4$	6.7(2)	−3.4(1)	7.5(2)	5.8
					$Ho1^2$, $Ho1^3$, $Ho3^2$, $Ho3^3$	6.7(2)	3.4(1)	7.5(2)	
					$Ho2^1$, $Ho2^4$	4.9(1)	5.7(2)	7.5(2)	
					$Ho2^2$, $Ho2^3$	4.9(1)	−5.7(2)	7.5(2)	
10	1.1252(2)	0.41411(5)	1.1111(2)	4.4	$Ho1^1$, $Ho1^4$, $Ho3^1$, $Ho3^4$	7.9(2)	−4.0(1)	8.9(2)	5.8
					$Ho1^2$, $Ho1^3$, $Ho3^2$, $Ho3^3$	7.9(2)	4.0(1)	8.9(2)	
					$Ho2^1$, $Ho2^4$	4.9(1)	7.4(2)	8.9(2)	
					$Ho2^2$, $Ho2^3$	4.9(1)	−7.4(2)	8.9(2)	
1.5	1.1248(2)	0.41409(5)	1.1111(2)	5.3	$Ho1^1$, $Ho1^4$, $Ho3^1$, $Ho3^4$	8.0(2)	−4.3(1)	9.1(2)	6.0
					$Ho1^2$, $Ho1^3$, $Ho3^2$, $Ho3^3$	8.0(2)	4.3(1)	9.1(2)	
					$Ho2^1$, $Ho2^4$	4.8(1)	7.7(2)	9.1(2)	
					$Ho2^2$, $Ho2^3$	4.8(1)	−7.7(2)	9.1(2)	

[a] X-ray data used with permission - © JCPDS - International Center for Diffraction Data.

5. Conclusions

The mixed antiferromagnetic–ferromagnetic nature of La_3NiGe_2-type Ho_3NiGe_2 is evident both from the magnetization and neutron diffraction studies. Analysis of the powder neutron diffraction data reveals that the Ho_3NiGe_2 phases exhibit a commensurate *ac*-plane ordering of the holmium sublattice with the **Pn'ma** magnetic space group. Below the magnetic transition temperature the *a* and *c* cell parameters of Ho_3NiGe_2 decrease whereas the *b* one remains almost constant.

Acknowledgments

The Institute Laue Langevin is warmly acknowledged for the use of the neutron diffraction beam. This work is supported by an ICDDGrant no.05-07.The crystallographic data of Ho_3NiGe_2 were used with permission - © JCPDS - International Center for Diffraction Data. This work was supported by the *Russian Fund for Basic Research* through the Project no.12-03-00428-a.

References

[1] Pearson's Handbook of Crystallographic Data for Intermetallic Phases, American Society for Metals, Metals Park, OH (1985) 1–3.
[2] P. Manfrinetti, A.V. Morozkin, O. Isnard, F. Wrubl, Y. Mozharivskyj, V. Svitlyk, Intermetallics 19 (2011) 321–326.
[3] A.V. Morozkin, Jinlei Yao, Y. Mozharivskyj, O. Isnard, J. Magn. Magn. Mater. 324 (2012) 2977–2982.
[4] F. Izumi, in: R.A. Young (Ed.), "The Rietveld Method", Oxford University Press, Oxford, 1993 (Chap. 13).
[5] Yellow Book, ⟨www.ill.eu⟩.
[6] J. Rodriguez-Carvajal, Physica B 192 (1993) 55–69.
[7] J. Emsley, The Elementssecond edition, Clarendon press, Oxford, 1991.
[8] S. Legvold, Rare earth metals and alloys, in: E.P. Wohlfarth (Ed.), Ferromagnetic Materials, North-Holland Publishing Company, Amsterdam, 1980, pp. 183–295.
[9] P.S. Kireev, Introduction to the theory group and it's application in solid state physic, Moscow, High School: 1979 (In Russian).
[10] C.J. Bradley, A.P. Cracknell, The Mathematical Theory of Symmetry in SolidsClarendon, Oxford, 1972.
[11] O.V. Kovalev, Representations of the Crystallographic Space Groupssecond edition, Gordon and Breach Science Publishers, 1993.
[12] S.F. Matar, B. Chevalier, O. Isnard, J. Etourneau, J. Material Chemistry 13 (2003) 916–920.